Climate Change Extreme Wind Effects on Transmission Towers

First author

Panagiotis Manis MEng (Hons) MSc (Eng)
Civil/Structural Engineer - Bridges & Civil Structures
Ove Arup and Partners Ltd
4 Pierhead Street
Capital Waterside
Cardiff CF10 4JB

Second (corresponding) author:

Alan G. Bloodworth MA MSc DIC DPhil CEng MICE
Principal Teaching Fellow in Civil Engineering
School of Engineering
University of Warwick
Library Road
Coventry CV4 7AL
Email: A.Bloodworth@warwick.ac.uk

Abstract

Climate change poses a major threat to electricity power infrastructure due to expected increase in magnitude and frequency of extreme storm events. This paper uses a methodology for assessment of the vulnerability of UK transmission tower infrastructure to such events, within a framework of performance based engineering.

The challenge of estimating future storm magnitudes is addressed by applying a Change Factor Methodology to present day wind speeds using information provided by 2009 UK Climate Change Projections. A Weibull distribution is employed to obtain wind speeds for storm events at different recurrence intervals. Wind loading on the structure and cables is then determined using Eurocodes, and the structure analysed by pseudo-static finite element analysis, considering material and geometrical nonlinearity as well as linear and nonlinear buckling effects.

The outcome of the research is that despite a significant projected increase in wind velocities due to climate change, the typical tower analysed in the study continues to perform satisfactorily at all hazard levels. If this performance can be demonstrated more generally across the UK transmission tower infrastructure network, then it is likely that the cause can be traced back to the high factor of safety applied in the original design of the towers.

Keywords: Steel structures; Wind loading & aerodynamics; Risk & probability analysis

List of Symbols

Roman Symbols

AEP	Annual exceedance probability
B^2	Background factor
B	Average width of the transmission line tower $[m]$
$\overline{CF}_{add,m}$	Additive change factor for baseline period mean wind speed for month m $[m/s]$
$C_{f,\theta}$	Force (or drag) coefficient for wind incidence angle θ without considering free-end flow
c	Weibull scale parameter $[m/s]$
c_b	Weibull scale parameter (baseline period) $[m/s]$
c_d	Dynamic factor
c_p	Weibull scale parameter (future period) $[m/s]$
c_s	Size factor
$c_s c_d$	Structural factor
E	Emissions scenario
f_1	Fundamental (first) natural frequency $[Hz]$
$f_L(z,f)$	Dimensionless frequency based on height z and frequency f
f_n	Natural frequency for the n-th mode $[Hz]$
$F(V)$	Cumulative distribution function (CDF)
H	Total height of the transmission line tower $[m]$
i	Measurement interval of wind speed observations
$I_v(z)$	Turbulence intensity at height z
k	Weibull shape parameter
k_I	Turbulence factor
k_p	Peak factor
$L(z_s)$	Turbulent length scale at the reference height z_s $[m]$
L_c	Length of transmission line cables $[m]$
m	Number of month under consideration

m_c	Mass per unit length of the cable $[m]$
n	Number of non-zero wind speed observations
P	Probability level for cumulative distribution function (CDF)
q_p	Peak velocity pressure acting on a structure or structural component $[N/m^2]$
q_w	Wind pressure acting on a structure or structural component $[N/m^2]$
R	Region
R^2	Resonance factor
$R_B(\eta_B)$	Aerodynamic admittance function for width B
$R_H(\eta_H)$	Aerodynamic admittance function for height H
RI	Recurrence interval $[years]$
$R_x(\eta_x)$	Aerodynamic admittance function for dimension x
$S_L(z,f)$	Power spectral density function at height z and natural frequency f
T	Future time period
T_c	Tensile load in transmission line cables $[N]$
V	Wind speed $[m/s]$
$\bar{V}$	Mean wind speed $[m/s]$
$\bar{V}_{b,m}$	Baseline period mean wind speed for month m $[m/s]$
$\bar{V}_{b,max}$	Maximum baseline period mean wind speed $[m/s]$
V_i	Wind speed measured at interval i $[m/s]$
$V_m(z)$	Mean wind velocity $[m/s]$
$\bar{V}_{p,m}$	Projected mean wind speed for month m $[m/s]$
$\bar{V}_{p,max}$	Maximum projected mean wind speed $[m/s]$
z	Height above ground level $[m]$
z_{min}	Minimum height for terrain category II $[m]$
z_0	Roughness length $[m]$
z_s	Reference height for structural factor $[m]$
$z_{s,c}$	Reference height for transmission line cables $[m]$
$z_{s,t}$	Reference height for transmission line tower $[m]$
z_t	Reference height for turbulence

Greek Symbols

α	Exponent factor for terrain category II
Γ	Gamma function
γ_Q	Partial safety factor for variable actions according to Eurocode
ζ	Total logarithmic decrement of damping
ζ_a	Logarithmic decrement of aerodynamic damping
ζ_s	Logarithmic decrement of structural damping
η_B	Variable required by the aerodynamic admittance function R_B
η_H	Variable required by the aerodynamic admittance function R_H
η_x	Variable required by the aerodynamic admittance function R_x
θ	Wind incidence angle [$degrees$]
λ	Effective slenderness
μ_e	Mass per unit area [kg/m^2]
ρ_{air}	Air density [kg/m^3]
φ	Solidity ratio
ψ_λ	End-effect factor

Introduction

Typhoon Haiyan in the Philippines in 2014 illustrated the vulnerability of power infrastructure to extreme wind loading events and consequential adverse effects on communities. This was also shown on a smaller scale in a succession of storms events in the UK early 2014 that damaged a transmission line tower in the northeast of England (Fig. 1) (BBC News, 2014). An increase in magnitude and frequency of extreme storm events in the UK is expected as a result of climate change (Natural England, 2009).

The high voltage transmission line network is a key element of the electrical power infrastructure (Ahmed, et al., 2010). The mainland UK network and location of nuclear power stations is shown in Figure 2. For this project, a critical area of the network strategically located between England and Scotland and close to two nuclear power stations was selected (marked with a red circle) to explore its vulnerability to climate change. Coincidentally, this is also the area of the Houghton-le-Spring failure (Fig. 1).

The electricity transmission network comprises transmission lines and two types of towers: suspension and tension. Suspension towers occur on straight sections of the network, supporting only the cables' self-weight and wind loading on them as well as the tower itself. Tension towers are placed at changes in line direction, subjected to additional forces induced by the cable tensions as a result of the direction change, and are thus heavier and more visually intrusive than suspension towers (GHD, 2013). Heights of both types of tower range from 40 – 50 m (National Grid, 2012), and all towers in the UK currently are of steel lattice type with angle members, a cost effective structural form for this purpose (Lomas, 1993).

Because most towers are of the suspension type, they were taken as the subject of this study. A particular D L6 Blaw Knox type tower located in Dorset was nominated as typical on the network (Fig. 3). The tower has a total height of 53 m and square base with side length 10 m, with six arms supporting 24 transmission cables (4 per arm) plus an earth wire at the top. Equal angle (EA) and unequal angle (UA) sections were utilised for its construction, ranging in size from 45x45x5 EA to 200x200x16 EA.

Performance of Transmission Towers in Extreme Storm Events

Extreme wind events have caused about 80% of tower failures in the USA, Australia, South Africa and other countries (Savory, et al., 2001; Dempsey & White, 1996), failures resulting in high costs for repair or reconstruction, as well as from power outages and litigation (Albermani, et al., 2009). 161 towers collapsed during the period 1948-2009 in the North-western USA (Xie & Sun, 2013) and similar events in Australia caused failure of more than 94 towers (Hawes & Dempsey, 1993). An extreme wind event in China in 2005 caused the collapse of more than 75 towers (Xie & Sun, 2013). In Europe, the *Lothar* and *Martin* windstorms of 26th-28th December 1999 caused 280 towers to fail, leading to power outages affecting 10 million people (RMS, 2002). More recently, the *Kyrill* windstorm of January 2007 was one of the most damaging events experienced in Northern Europe, causing the collapse of towers in the UK and across central Europe. These and other events led to the conclusion that climate change is expected to enhance the magnitude and frequency of extreme storm events (Rademaekers, et al., 2009) and that European standards for tower design need to be revised (Anagnostatos, et al., 2013).

Damage to transmission line networks may be associated with failure of the tower substructure (Richards, et al., 2010) or superstructure, or breakage of transmission lines (Pang, et al., 2013). This paper focusses on the superstructure of the towers. Substructure stiffness influences stresses in the superstructure, with spring supports reducing the maximum stresses (Newton, 2004). However, unless soil parameters are available with sufficient certainty at the site, foundations are usually taken as rigid, a safe assumption for the superstructure.

Failure under extreme wind loads has been investigated by means of numerical modelling and full- or large-scale model tests. In several such tests, it has been observed that tower failure under lateral loading is caused by flexural-torsional buckling of the main legs and diagonal bracing members and is normally confined to the bottom two stages of the tower (Xie & Sun, 2013). Transfer of bending moments to the diagonal bracing members at the joints with main leg members induces out-of-plane buckling of the bracing members. This causes the main members to lose restraint whilst simultaneously experiencing torsion due to the bracing out-of-plane deformations. This is affirmed by field observations from Germany, where some tower failures were caused by buckling of the main leg members as a result of failure of bracing members (Klinger, et al., 2011).

Performance Based Wind Engineering Framework

This paper aims to assess the vulnerability of UK transmission tower infrastructure within a Performance Based Wind Engineering (PBWE) framework. PBWE examines the adequacy of a structure for different "Hazard Levels" via the aid of "Decision Variables" and "Performance Objectives". (Ciampoli, et al., 2011).

Hazard Levels (HL) at a site are defined by the intensity or recurrence interval of wind events (Petrini, et al., 2009). For this project, five HL were considered: Frequent (2-3 years), Occasional (10 years), Rare (50-100 years, the usual basis for structural design), Very Rare (250 years) and Maximum Considered (500-1000 years).

Decision Variables (DV) are specific measures of the consequence of structural failure from the point of view of structure owners, users or wider society (Ciampoli, et al., 2011). Those applicable to electricity transmission towers are judged as follows:

- Large numbers of people and industries affected and put at risk by power outages;
- High costs arising from structural and non-structural damage, power outages and litigation;
- Long duration of repair or reconstruction works, further increasing discomfort.

These DV are used to decide the "Importance Level" of the structure, either Normal, Essential or Safety Critical. Normal importance is applicable when a small number of people might be affected by damage or failure, whereas Essential is when a large number of people are affected (*e.g.* hospitals, schools). Safety Critical is appropriate for nuclear facilities or structures storing toxic or explosive materials (SEAOC, 1999). Transmission towers are judged to be of Essential importance.

Performance Objectives (PO) are assigned to each HL depending on the Importance Level of the structure. Four PO were defined following the philosophy of the performance-based seismic engineering

framework of SEAOC (1999), comprising two repairable damage states (Fully Operational and Operational) and two non-repairable (Damage Control and Near Collapse). Conceptually, the damage level for each PO may be described via either "Engineering Demand" parameters (*e.g.* displacement at a specific location of the structure) or "Damage Measure" parameters (DM) (*i.e.* allowable extent of damage) (Petrini, et al., 2009). In this project DM parameters were used to simplify the framework, determined as follows:

- **Negligible Damage (Fully Operational):** No yielding or buckling of structural elements at any location of the structure
- **Slight Damage (Operational):** Slight yielding or buckling of a small number of elements causing some permanent deformations. Structure remains operational, no power outages, and damage might be economically repairable without significant disruption.
- **Moderate/Heavy Damage (Damage Control):** Significant yielding or buckling of a considerable number of structural elements, with large deformations although a margin maintained against onset of collapse (no mechanism formed). Structure no longer operational and damage usually not economically repairable.
- **Severe Damage (Near Collapse):** Severe yielding or buckling of a large number of critical structural elements (*e.g.* main leg members). Gravity loads may still be supported by the structure but formation of a mechanism highly likely, leading to partial or total collapse.

The damage to the structure at each HL is estimated by numerical simulation and compared with the allowable extent of damage for each PO to evaluate the structural performance (Petrini, et al., 2009). A framework for making these comparisons is given in Table 1. As HL increases, the required performance level decreases, and for a given HL, as Importance Level increases, the required performance level increases. If allowable damage is exceeded for a particular HL, the structure has failed to meet its PO, indicated 'Unacceptable'. For transmission towers (Essential importance), slight damage is considered acceptable under Rare storm events, moderate/heavy damage for a Very Rare storm and severe damage for Maximum Considered events.

Magnitude and Frequency of Future Extreme Wind Events

The input to the PBWE framework in Table 1, *i.e.* the Hazard Levels, are magnitudes of future extreme storm events at different return periods. The only reliable future wind projections currently available for the UK are contained in the open access 2009 UK Climate Projections (UKCP09) resource (UKCP, 2012a), produced using the Met Office Hadley Centre Coupled Model 3 (HadCM3) and a weather generator (Sexton & Murphy, 2010). HadCM3 is an Atmosphere-Ocean Global Circulation Model that recognises the significant influence that oceanic processes have on the atmosphere (UKCP, 2012b). The weather generator produces a long time series of future climate data from past weather observations over a baseline period, 1961-1990 (UKCP, 2012c).

UKCP09 does not attempt to provide absolute projections of future wind speed or direction, due to lack of robustness of the dataset (Eames, et al., 2011). Instead, projections of *changes* in mean wind speed relative to the 1961-1990 period can be extracted for certain emissions scenarios (Murphy, et al., 2009) from data files of Batch 3 of the "*UK Probabilistic Projections of Climate Change over Land"* accessible

via the UKCP09 User Interface (UKCP UI, 2012). These projected changes require statistical manipulation involving the Change Factor Method (CFM) to compute mean and extreme future wind speeds.

UKCP09 data files are grouped with respect to location, future time period, emissions scenario and temporal averaging period. For location, the UK is divided into 16 administrative regions. There are seven future overlapping time periods from 2010-2039 to 2069-2099, of 30-year duration to reduce uncertainties from variability in natural internal processes within the climate system (Jenkins, et al., 2009). Three emission scenarios have been extracted from the Special Report on Emission Scenarios by the Intergovernmental Panel on Climate Change, namely High (A1FI), Medium (A1B) and Low (B1) (Warren, 2010). All projections are provided for three temporal averaging periods – monthly, seasonal and annual (Jenkins, et al., 2009) and are probabilistic, comprising Cumulative Distribution Function (CDF) data of changes in mean wind speeds over 107 pre-defined probability levels, from 1% to 99.9 % (UKCP, 2012d).

The critical area of the transmission line network considered in this paper is in administrative region (R) North East England (NEE). The 2080s (2069-2099) time period (T) was chosen to maximise climate change effects on the towers. In terms of emissions scenarios (E), Low (B1) is considered unlikely, given current carbon emissions (Eames, et al., 2010). Medium and High both belong to the A1 family; High results from intensive use of fossil fuels (FI), which is quite conservative and so Medium emissions (A1B) was assumed, where 'B' denotes 'balanced' use of fossil and non-fossil energy sources. The accuracy of projections decreases as the temporal scale increases, so a monthly averaging period was selected. Finally, the probability level (P) for projected changes in mean wind speeds was taken as 95%, typical for determination of characteristic actions on structures.

In the CFM there are several change factor types, classified with respect to their temporal scale, temporal resolution, mathematical basis (additive or multiplicative) and number (single or multiple) (Anandhi, et al., 2011). Temporal scale is related to the temporal averaging period of the data files, either daily, monthly, seasonal or annual. Temporal resolution is associated with time of year as well as start and end dates of the historical and future observations. Additive change factors quantify the differences between current and projected future values while multiplicative factors express the ratio of future values to current values. Single change factors remain unchanged for all possible values or probability levels of a variable (Hay, et al., 2000), whilst multiple change factors have to be computed separately (Kilsby, et al., 2007).

As stated earlier, a monthly temporal averaging period was selected to maximise the accuracy of the results. Temporal resolution is determined in the UKCP09 data files that are produced for a specific baseline period and selected 30-year future time periods. In order to avoid inheriting variations from the long-term average, the period of weather data observations should not be less than 30 years (Lun & Lam, 2000). UKCP09 projections for changes in mean wind speeds from the baseline period are inherently additive change factors, and are provided for different percentiles via the aid of a CDF, indicating the presence of multiple change factors for each month. Therefore, the CFM in this project uses multiple monthly additive change factors, and the following expression applies:

$$\bar{V}_{p,m} = \bar{V}_{b,m}(R) + \overline{CF}_{add,m}(R,T,E,P) \quad (1)$$

where m is the month under consideration, $\bar{V}_{p,m}$ is the projected future mean wind speed for month m, and

$\bar{V}_{b,m}$ the baseline period mean wind speed for month m for the selected region R available on the Met Office website (Met Office, 2013). $\overline{CF}_{add,m}$ is the additive change factor for month m, which is dependent on selected region R, future time period T, emissions scenario E and desired CDF probability level P.

After calculating projected future mean wind speeds for all 12 months of the year using Equation (1), the maximum mean monthly wind speed is selected for both baseline and future periods. These maxima are used for determination of future extreme storm event magnitudes. For the region under consideration, the maximum baseline mean wind speed ($\bar{V}_{b,max}$) was computed as 11.54 m/s in January (month 01) and the maximum future projected mean wind speed calculated:

$$\bar{V}_{p,max} = \bar{V}_{p,01} = \bar{V}_{b,01}(NEE) + \overline{CF}_{add,01}(NEE, 2080s, MED, 0.95) = 11.54 + 0.20 = 11.74\ m/s \qquad (2)$$

Having obtained a projection of future maximum mean monthly wind speeds, the next stage is to extend the analysis to extreme wind events. This is normally done statistically with Extreme Value Theory, based on the Generalised Extreme Value (GEV) distribution (Chiodi & Ricciardelli, 2014). However, to determine the parameters of the GEV distribution, extreme wind data should be utilised (Xiao, et al., 2006). Considering that only projections of future mean wind speeds are available, not extreme values, it is deduced that extreme value distributions are not appropriate for this case.

On the other hand, the two-parameter Weibull distribution is reasonably robust for representing both mean and extreme wind speed data (Chiodi & Ricciardelli, 2014) and may be used to obtain estimates of extreme wind speeds from mean wind speeds provided plausible values for the Weibull parameters can be obtained. Even though fitting a Weibull distribution is an empirical method, it produces results very close to the Offset Elliptical Normal model which has a strong theoretical background, over the range of practical values (Harris & Cook, 2014).

The PDF and CDF of the Weibull distribution are (Lun & Lam, 2000):

$$\text{PDF:} \quad f(V) = \begin{cases} \frac{k}{c}\left(\frac{V}{c}\right)^{k-1} e^{-\left(\frac{V}{c}\right)^{k}} & if \quad x \geq 0 \\ 0 & if \quad x < 0 \end{cases} \qquad (3)$$

$$\text{CDF:} \quad F(V) = \left[1 - \exp\left(-\left(\frac{V}{c}\right)^{k}\right)\right] \qquad (4)$$

Where V is the wind speed, c the scale parameter and k the shape parameter. The smaller k, the greater the deviation of wind speeds from the mean, implying more extreme events. A relationship between the two Weibull parameters has been established (Seguro and Lambert, 2000):

$$\bar{V} = c \cdot \Gamma\left(1 + \frac{1}{k}\right) \qquad (5)$$

Where $\bar{V}$ is the mean wind speed, and Γ the gamma function.

Although Weibull parameters cannot be obtained from the UKCP09 data directly because it provides projections only of future mean wind speeds, they may be computed from recorded wind speed data if the assumption is made that the same distribution of wind speeds will apply in the future. Recorded data is available for the UK from the British Atmospheric Data Centre (BADC) and the Natural Environment Research Council (NERC) "*Met Office Integrated Data Archive System (MIDAS) Land and*

Marine Surface Stations" datasets, which provide hourly mean wind speeds for the period 1853 to the present for several locations (BADC & NERC, 2011). Although data is available from the 1961-1990 baseline period, there were more weather stations in the UK from the 1970s onwards, so the 1971-2005 period was used instead.

There are several methods by which shape parameter k can be computed from a set of hourly wind speed data. The Maximum Likelihood Method (MLM) has been found to provide reasonably accurate estimates (Kaoga, et al., 2014; Ahmed, 2013) provided wind data are available in time series format (Seguro & Lambert, 2000), which is the case for this project. According to the MLM, k can be computed as follows:

$$k = \left(\frac{\sum_{i=1}^{n} V_i^k \ln V_i}{\sum_{i=1}^{n} V_i^k} - \frac{1}{n} \sum_{i=1}^{n} \ln V_i \right)^{-1} \tag{6}$$

Where n is the number of non-zero wind speed observations, i the measurement interval (one hour) and V_i the wind speed at time interval i.

The only location in northeast England with at least 30 years of wind speed observations is Durham (MIDAS Station 326). Using its 1971-2005 data, k computes as 1.28, and the fit of the Weibull distribution to the data is shown in Figure 4. All zero values are replaced by 0.5 knots (0.25 m/s), the threshold below which wind speed measurements are recorded as zero (Young, 2010).

The fit of the Weibull PDF with k = 1.28 to the recorded data is good, especially at high wind speeds. By substituting mean wind speed and k into Equation (5), the scale parameter c for the baseline and future time periods can be determined (Table 2) and PDFs for both periods plotted (Figure 5). The distributions for the baseline and future time periods are similar in shape (as the same shape parameter k is used), but there is a decrease in the future in the probability of wind speeds up to 15 m/s and an increase in the probability of speeds higher than 15 m/s, indicating climate change causing an increase in magnitude and frequency of future extreme storm events.

Recurrence Intervals for Future Wind Speeds

The probability of occurrence of a specified wind speed provides input to the PBWE framework (Table 1). The annual exceedance probability (AEP) of a specified wind speed is directly related to the CDF of the Weibull distribution (USGS, 2014):

$$AEP = 1 - F(V) \tag{7}$$

Recurrence interval (RI) in years is the inverse of the AEP, hence:

$$F(V) = 1 - 1/RI \tag{8}$$

Substituting Equation (8) into (4) and after some manipulation, an expression relating wind speed and RI can be derived:

$$V = c\left(-\ln\frac{1}{RI}\right)^{1/k} \tag{9}$$

By substituting Weibull parameters c and k into Equation (9), future hourly mean wind speeds with recurrence intervals corresponding to the PBWE Hazard Levels are determined. These are compared with the baseline 1961-1990 data in Table 3. At longer RI, wind speeds are considerably higher, suggesting the possibility of catastrophic structural damage.

To summarise, the methodology followed to determine the magnitude of future extreme storm events is presented in the form of a flowchart in Figure 6.

Wind Loading Calculations

Future wind speeds obtained by the methodology described above were used to obtain the wind loads on the transmission tower using the procedure in Eurocode 1 Part 1-4 (BSI, 2005). This applies an amplification factor to account for dynamic response of the structure due to effects of wind turbulence, so that pseudo-static analysis is sufficient to assess the tower's performance.

Future hourly mean wind speeds are converted first to 10-minute mean wind speeds for input into the Eurocodes. Durst (1960) developed a non-hurricane wind gust duration curve giving relationships between wind speeds averaged over arbitrary intervals to the 1-hour mean wind speed (Tamura & Kareem, 2013). According to this curve, the 10-minute mean wind speed is approximately 7% larger than the hourly mean, and applying this factor to the future hourly mean wind speeds presented in Table 3, future 10-minute wind speeds are obtained (Table 4).

A typical wind loading profile was taken, with wind speed increasing with height for two wind incidence angles: 0° and 45° from the normal to the front face of the tower. 45° incidence transpires to be most adverse because the reference (frontal) area of the structure is larger, and the wind-induced overturning moment is resisted by only two out of the four main legs of the tower in opposing corners on the diagonal parallel to the wind (Fig. 7). More detail of the steps in the wind load calculation and the values of certain variables used are given in the Appendix.

Structure assessment philosophy and modelling strategy

A basic dynamic analysis of a lattice structure would assume linear elastic behaviour, with connections considered as pinned and members assumed subjected to axial loading only (ArcelorMittal, 2010). However, full scale transmission tower tests have shown that bending stresses in some members can be as high as axial stresses (Albermani & Kitipornchai, 2003), and that nonlinear effects should be taken into account (Albermani, et al., 2009).

Most connections in towers have multiple high-strength friction grip bolts leading to a high degree of restraint, which although not significantly changing axial force magnitudes, does give rise to secondary

bending moments (ArcelorMittal (2010)). Connections should therefore be modelled as rigid and members with beam-column elements (Battista, et al., 2003; Albermani, et al., 2009). Slip theoretically may occur in bolted connections and including it in an analysis has been shown to improve prediction of tower deformations, but not affect load-bearing capacity or failure mode significantly (Eltaly, et al., 2014; Jiang, et al., 2011). Hence, joint slip was not included in this study.

The two main sources of nonlinearity are (Eltaly, et al., 2014; Jiang, et al., 2011):

- Geometric nonlinearity that accounts for the effect of changes in geometry and accumulated strain on the structural stiffness of elements (Hrinda, 2006)
- Material nonlinearity that accounts for permanent (or plastic) deformation in materials subjected to stresses exceeding their yield point (Souza Neto, et al., 2008)

To determine the dynamic response of the towers accurately, wind-induced response of the transmission lines should also be included in the model (Zhang, et al., 2013; Battista, et al., 2003). Although a model with three towers and four spans of transmission lines is the optimal configuration for analysis (Zhang, et al., 2013), one tower and two spans of transmission lines can produce reasonably accurate results with enhanced computational efficiency (Li, et al., 2012).

Fatigue failure is not analysed in this study because the focus of the study is on survivability under extreme loading events. The general increase in wind loading predicted due to climate change would be expected to increase the stress ranges acting on fatigue-critical elements or connections, and thus shorten the service life of the structure.

Numerical Modelling Implementation

The LUSAS Finite Element Analysis program was used (LUSAS, 2015). Tower geometry was available from a previous research project that utilised drawings provided by National Grid (Tyndel, 2006). Elements were assigned as thick nonlinear three-dimensional (3D) beams (BTS3), which support materially and geometrically nonlinear and linear eigenvalue buckling analyses. BTS3 is compatible with a stress resultant material model (Model 29) for material nonlinearity (hardening behaviour of materials is not supported), and co-rotational formulation for geometric nonlinearity (large displacements and rotations, small strains).

All beam ends (and foundation supports) were set as fully restrained to model rigid connections. An element discretisation length of 0.05 m was determined after carrying out a mesh sensitivity analysis to minimise load factor. Geometric properties of the elements were assigned from the in-built section library of UK equal and unequal angles. Crucially, the orientation of all elements in the model was set according to the tower drawings. A view of the resulting model for the base of a main leg member is shown in Figure 8.

Yield strength of steel was taken as 275 N/mm^2. Young's modulus, Poisson's ratio and mass density were set as 209 GPa, 0.3 and 7800 kg/m^3 respectively. Loading applied to the tower included gravity on all structural elements, together with concentrated loads on the arms to account for self-weight of

the cables and wind-induced forces on them. Wind load on the structural elements was applied using uniform Global Distributed Loads, with half of the calculated wind load applied to the front face(s) of the tower and the remainder to the back.

Modelling Results

The transmission tower model was analysed numerically for the three Hazard Levels of Rare, Very Rare and Maximum Considered (Table 4). Results are presented in the form of an overall load factor. If this is considerably larger than 1.0, there are no concerns with the performance of the structure, but if close to or smaller than 1.0, then scrutiny is required before a decision is made.

Material and Geometrically Nonlinear Analyses

Load factors obtained considering material nonlinearity (MNL), and material and geometric nonlinearity (MGNL), are presented at Table 5. Analyses halted when only a small number of elements had yielded, not with formation of a collapse mechanism, due to inability of the Stress Resultant material model to support post-yield hardening behaviour of materials. Smallest load factors were obtained from the MGNL analyses for 45° wind incidence. For a Rare event ($RI = 50$ years), the lowest overall load factor is 1.06, indicating no damage and the structure remaining Fully Operational (Table 1). It was also found (not shown in Table 5) that for a Rare event with RI = 100 years, the load factor reduces to 0.87 indicating the structure experiencing slight damage (yielding of a small number of elements) but remaining Operational. Thus the structure meets its PO for Rare storm events.

For Very Rare and Maximum Considered events, smallest load factors are 0.63 and 0.52 respectively. It is therefore necessary to investigate further the post-yielding behaviour of the structure. A pushover analysis was performed for the Very Rare event ($RI = 250$ years) under 45° wind. Load factor against top deflection of the tower is shown in Figure 9.

Up to point 1 (*i.e.* Analysis 1) in Figure 9, the structure behaved linear elastically. The load factor peaks at point 2, with significant deflection due to yielding of one of the main leg members. Between points 2 and 6, there is a reduction of approximately 60% in load factor with large increase in deflection. Usually, 20-30% loss of peak strength is considered as structure failure, hence the structure can be viewed here as severely damaged. At point 7, a small increase in strength is observed. The main leg members on the diagonal in the direction of the wind have yielded, and the other two legs start to resist a portion of the applied loads. However, they are much less efficient at resisting overturning, so the structure strength decreases thereafter to only 15% of peak by point 12, accompanied by large deformations indicating the onset of collapse. The evolution of yielding for points 2, 7 and 11 is shown in Figure 10 and the deformed shape at the end of the analysis in Figure 11 from four different views. Displacements are not exaggerated in scale and there is approximately 5.5 m displacement at the top.

The pushover analysis applied maximum wind loading as a steady force until failure was induced. In reality however, wind storm loading is not a steady force but contains gusts with duration 2-3 s. Also,

during yielding of members of the structure, there is significant energy dissipation due to formation of plastic hinges. Therefore, the pushover analysis will overestimate the damage to the structure, which would probably experience moderate/heavy damage but without collapse. Thus, the Damage Control PO (Table 1) is likely to be satisfied for the Very Rare event. Under the Maximum Considered ($RI = 500$ years) event, the structure would be closer to collapse under the load factor of 0.52, in agreement with the PO Near Collapse.

Linear Eigenvalue Buckling Analyses

A linear eigenvalue buckling analysis determines the maximum load that can be sustained by the structure before structural instability occurs. Table 6 shows the resulting load factors for the first two global buckling modes, both of which involve out-of-plane buckling of the diagonal bracing elements in the bottom stage of the structure (Fig. 12). A mode with lower load factors exists but comprises buckling of only one member and is not critical for collapse of the structure. As for the MNL and MGNL analyses, lowest load factors are obtained for the 45° wind incidence angle.

Table 6 shows that for the Rare storm, the structure remains Fully Operational as all load factors are significantly larger than 1.0. For the Very Rare event, all load factors are larger than or equal to 1.0, implying that the structure would at most experience only slight damage and remain Operational, again exceeding the required PO. For the Maximum Considered event, three of the four load factors are smaller than 1.0. The buckling mode shown in Figure 13 would induce torsion in and reduce restraint to the main leg members and likely lead to their flexural-torsional failure, as observed in full scale tests noted earlier in this paper. The structure would experience severe damage and potentially complete collapse. However, this meets the PO for that Hazard Level which is Near Collapse.

Nonlinear Buckling Analyses

A buckling analysis taking into account material and geometric nonlinearity effects was also performed. However, because the critical failure mode identified by the materially and geometrically nonlinear analyses is similar to that in the linear buckling analyses, similar results were obtained when all the effects were combined.

Summary of Vulnerability of UK Transmission Tower Infrastructure

A summary of the performance of the example transmission tower deduced from this research is given in Table 7. Even though climate change is projected to significantly increase extreme wind velocities, tower performance is satisfactory for all Hazard Levels.

Conclusions

This paper has used a methodology for estimating the magnitude of future extreme wind speeds by means of a change factor methodology in which recorded mean wind speeds from a past 30 year baseline period are uplifted by amounts proposed in the open access 2009 UK Climate Projections resource. Hourly mean wind speeds for a range of recurrence intervals are then obtained using a Weibull distribution in which a

necessary assumption is made that the Weibull parameters for future events will be the same as for past historical data. Wind loading on a typical transmission tower is then calculated using established Eurocode methodologies and the tower modelled and structurally assessed within a framework of performance-based engineering, in which appropriate performance levels or damage are sought at different input hazard levels. Performance of the tower was satisfactory at all hazard levels. The tower modelled is typical on a network where a factor of safety of 2.5 was applied in the original design to enhance reliability during adverse weather conditions (Lomas, 1993). It appears that this original safety allowance has given sufficient robustness to the network under projected increased storminess due to climate change.

Acknowledgements

Provision of transmission tower drawings by National Grid is acknowledged with thanks. The advice of former colleagues at the University of Southampton, Professor Patrick James and Professor Adrian Chandler, is appreciated. Views expressed in this paper are those of the authors only.

References

Ahmed, A., Arthur, C. & Edwards, M., 2010. "Collapse and Pull-down Analysis of High Voltage Electricity Transmission Towers Subjected to Cyclonic Wind". *IOP Conference Series: Materials Science and Engineering,* 10(1).

Ahmed, S. A., 2013. "Comparative Study of Four Methods for Estimating Weibull Parameters for Halabja, Iraq". *International Journal of Physical Sciences,* 8(5), pp. 186-192.

Albermani, F. & Kitipornchai, S., 2003. "Numerical Simulation of Structural Behaviour of Transmission Towers". *Thin-Walled Structures,* Volume 41, pp. 167-177.

Albermani, F., Kitipornchai, S. & Chan, R. W. K., 2009. "Failure Analysis of Transmission Towers". *Engineering Failure Analysis,* Volume 16, pp. 1922-1928.

Anagnostatos, S. D., Halevidis, C. D., Polykrati, A. D. & Bourkas, P. D., 2013. "Examination of the 2006 Blackout in Kefallonia Island, Greece". *Electrical Power and Energy Systems,* Volume 49, pp. 122-127.

Anandhi, A. et al., 2011. "Examination of Change Factor Methodologies for Climate Change Impact Assessment". *Water Resources Research,* 47(3).

ArcelorMittal, 2010. *"Design Manual - Steel Buildings in Europe - Single-Storey Steel Buildings - Part 5: Detailed Design of Trusses".* [Online]
Available at: http://sections.arcelormittal.com/fileadmin/redaction/4-Library/4-SBE/EN/SSB05_Detailed_Design_of_Trusses.pdf
[Accessed 27th July 2014].

BADC & NERC, 2011. *"Met Office Integrated Data Archive System (MIDAS) Land and Marine Surface Stations Data (1853-current)".* [Online]
Available at: http://badc.nerc.ac.uk/view/badc.nerc.ac.uk__ATOM__dataent_ukmo-midas
[Accessed 20 June 2014].

Battista, R. C., Rodrigues, R. S. & Pfeil, M. S., 2003. "Dynamic Behaviour and Stability of Transmission Line Towers under Wind Forces". *Journal of Wind Engineering and Industrial Aerodynamics,* Volume 91, pp. 1051-1067.

BBC News, 2014. *"In Pictures: Storms Batter UK".* [Online]
Available at: http://www.bbc.co.uk/news/in-pictures-26169252
[Accessed 20th February 2014].

BSI, 2005. *"Eurocode 1: Actions on Structures - General Actions - Part 1-4: Wind Actions (BS EN1991-1-4:2005)".* London, UK: British Standards Institution (BSI).

BSI, 2008. *"UK National Annex to Eurocode 1 – Actions on Structures – Part 1-4: General Actions – Wind Actions (NA to BS EN1991-1-4:2005)".* London, UK: British Standards Institution (BSI).

Burgess, I., Green, A. & Abu, A., 2010. *"Concise Eurocodes: Loadings on Structures (BS EN 1991: Eurocode 1)".* London, UK: British Standards Institution (BSI).

Chiodi, R. & Ricciardelli, F., 2014. "Three Issues Concerning the Statistics of Mean and Extreme Wind Speeds". *Journal of Wind Engineering and Industrial Aerodynamics,* Volume 125, pp. 156-167.

Ciampoli, M., Petrini, F. & Augusti, G., 2011. "Performance-Based Wind Engineering: Towards a General Procedure". *Structural Safety,* Volume 33, pp. 367-378.

Durst, C. S., 1960. "Wind Speeds over Short Periods of Time". *The Meteorological Magazine,* Volume 89, pp. 181-186.

Eames, M., Kershaw, T. & Coley, D., 2010. *"Weather Generator Read-me File".* Exeter, UK: University of Exeter.

Eames, M., Kershaw, T. & Coley, D., 2011. "The Creation of Wind Speed and Direction Data for the Use in Probabilistic Future Weather Files". *Building Services Engineering Research Technologies,* 32(2), pp. 143-158.

Eltaly, B., Saka, A. & Kandil, K., 2014. "FE Simulation of Transmission Tower". *Advances in Civil Engineering,* Volume 2014, pp. 1-13.

GHD, 2013. *"Wandoan South to Eurombah Transmission Network Project".* [Online]
Available at: http://www.ghd.com/pdf/421667705_B%20Chapter%203%20Part%203.pdf
[Accessed 26th June 2014].

Harris, R. I. & Cook, N. J., 2014. "The Parent Wind Speed Distribution: Why Weibull?". *Journal of Wind Engineering and Industrial Aerodynamics,* Volume 131, pp. 72-87.

Hawes, H. & Dempsey, D., 1993. "Review of Recent Australian Transmission Line Failures due to High Intensity". *Proceedings of the Task Force of High Intensity Winds on Transmission Lines.*

Hay, L. E., Wilby, R. L. & Leavesley, G. H., 2000. "A Comparison of Delta Change and Downscaled GCM Scenarios for Three Mountainous Basins in the United States". *Journal of the American Water Resources Association,* 36(2), pp. 387-397.

Hendry, C., 2005. *"The Behaviour of a Transmission Tower due to Extreme Wind Loading".* Southampton, UK: University of Southampton.

Hrinda, G. A., 2006. *"Geometrically Nonlinear Static Analysis of 3D Trusses Using the Arc-Length Method",* Hampton, VA, United States : NASA Technical Reports Server.

Jenkins, G. J. et al., 2009. *"UK Climate Projections: Briefing Report".* Exeter, UK: Met Office Hadley Centre.

Jiang, W. Q. et al., 2011. "Accurate Modeling of Joint Effects in Lattice Transmission Towers". *Engineering Structures,* Volume 33, pp. 1817-1827.

Kaoga, D. K., Raidandi, D., Djongyang, N. & Doka, S. Y., 2014. "Comparison of Five Numerical Methods for Estimating Weibull Parameters for Wind Energy Applications in the District of Kousseri, Cameroon". *Asian Journal of Natural & Applied Sciences,* 3(1), pp. 72-87.

Kilsby, C. G. et al., 2007. "A Daily Weather Generator for Use in Climate Change Studies". *Environmental Modelling & Software,* Volume 22, pp. 1705-1719.

Klinger, C. et al., 2011. "Failure Analysis on Collapsed Towers of Overhead Electrical Lines in the Region Münsterland (Germany) 2005". *Engineering Failure Analysis,* Volume 18, pp. 1873-1883.

Li, Q., Junjian, Y. & Wei, L., 2012. "Random Wind-induced Response Analysis of Transmission Tower-line System". *Energy Procedia,* Volume 16, pp. 1813-1821.

Lomas, C., 1993. "Transmission Tower Development in the UK". *Engineering Structures,* 15(4), pp. 277-288.

Lun, I. Y. F. & Lam, J. C., 2000. "A Study of Weibull Parameters Using Long-term Wind Observations". *Renewable Energy,* Volume 20, pp. 145-153.

LUSAS, 2015. *"LUSAS Finite Element Analysis - Engineering Analysis Software".* [Online]
Available at: http://www.lusas.com/
[Accessed 03 August 2015].

Met Office, 2013. *"UKCP09: Regional Averages".* [Online]
Available at:
http://www.metoffice.gov.uk/climatechange/science/monitoring/ukcp09/download/longterm/regional_values.html#monthly
[Accessed 12th June 2014].

Murphy, J. et al., 2009. *"UK Climate Projections Science Report: Climate Change Projections".* Exeter, UK: Met Office Hadley Centre.

National Grid, 2012. *"Electricity Transmission National Grid Assets".* Warwick, UK: National Grid Education.

Natural England, 2009. *"What Climate Change May Happen in the Future?".* [Online]
Available at:
http://www.naturalengland.org.uk/ourwork/climateandenergy/climatechange/whatis/Whatmayhappen.aspx
[Accessed 20th April 2014].

Newton, T., 2004. *"CENV3036 Individual Project - The Behaviour of a Transmission Tower due to Extreme Loading".* Southampton, UK: University of Southampton.

Pang, W., Chen, Z., Liu, F. & Holmes, R., 2013. "Failure Risk of 230kV Electricity Transmission Lines in South Carolina under Hurricane Wind Hazard". *Advances in Hurricane Engineering: Learning from Our Past - Proceedings of the 2012 ATC and SEI Conference on Advances in Hurricane Engineering,* pp. 840-850.

Petrini, F., Ciampoli, M. & Augusti, G., 2009. A probabilistic framework for Performance-Based Wind Engineering. *Proceedings of 5th European and African Conference on Wind Engineering (EACWE 5).*

Rademaekers, K. et al., 2009. *"Strengthening the EU Capacity to Respond to Disasters: Identification of the Gaps in the Capacity of the Community Civil Protection Mechanism to Provide Assistance in Major*

Disasters and Options to Fill the Gaps – A Scenario-based Approach". Rotterdam, Netherlands: ECORYS Research and Consulting.

Ren, W. X., Liu, H. L. & Chen, G., 2008. "Determination of Cable Tensions Based on Frequency Differences". *Engineering Computations: International Journal for Computer-Aided Engineering and Software,* 25(2), pp. 172-189.

Richards, D., White, D. & Lehane, B., 2010. "Centrifuge Modelling of the Pushover Failure of an Electricity Transmission Tower". *Canadian Geotechnical Journal,* 47(4), pp. 413-424.

RMS, 2002. *"Windstorms Lothar and Martin on December 26-28, 1999"*. California, USA: Risk Management Solutions, Inc.

Sá Caetano, E., 2007. *"Cable Vibrations in Cable-Stayed Bridges"*. Zurich, Switzerland: International Association for Bridge and Structural Engineering (IABSE).

Savory, E. et al., 2001. "Modelling of Tornado and Microburst-induced Wind Loading and Failure of a Lattice Transmission Tower". *Engineering Structures,* Volume 23, pp. 365-375.

SEAOC, 1999. *"Recommended Lateral Force Requirements and Commentary"*. 6th ed. SEAOC Seismology Committee: Structural Engineers Association of California (SEAOC).

Seguro, J. & Lambert, T., 2000. "Modern Estimation of the Parameters of the Weibull Wind Distribution for Wind Energy Analysis". *Journal of Wind Engineering and Industrial Aerodynamics,* Volume 85, pp. 75-84.

Sexton, D. M. H. & Murphy, J., 2010. *"UKCP09: Probabilistic Projections of Wind Speed"*. [Online] Available at: http://ukclimateprojections.metoffice.gov.uk/media.jsp?mediaid=87845&filetype=pdf [Accessed 20th March 2014].

Souza Neto, E. A., Peric, D. & Owen, D. R. J., 2008. *"Computational Methods for Plasticity: Theory and Applications"*. West Sussex, UK: John Wiley & Sons, Ltd.

Tamura, Y. & Kareem, A., 2013. *"Advanced Structural Wind Engineering"*. 1st ed. New York: Springer Japan.

Tubman, J. et al., 2010. *"Manual for the Design of Building Structures to Eurocode 1 and Basis of Structural Design"*. London, UK: The Institution of Structural Engineers.

Tyndel, A., 2006. *"The Behaviour of a Transmission Tower due to Extreme Wind and Ice Loading"*. Southampton, UK: University of Southampton.

UK Parliament, 2010. *"The Future of Britain's Electricity Networks - Energy and Climate Change"*. [Online]
Available at: http://www.publications.parliament.uk/pa/cm200910/cmselect/cmenergy/194/19404.htm [Accessed 12th June 2014]. Reproduced under the terms of the Open Government Licence v3.0 http://www.nationalarchives.gov.uk/doc/open-government-licence/version/3.

UKCP UI, 2012. *"UK Climate Projections - User Interface: CSV Archive"*. [Online]
Available at: http://ukclimateprojections-ui.metoffice.gov.uk/ui/start/start.php
[Accessed 14th June 2014].

UKCP, 2012a. *"UK Climate Projections: What is UKCP09?"*. [Online]
Available at: http://ukclimateprojections.metoffice.gov.uk/21678
[Accessed 20th April 2014].

UKCP, 2012b. *"UK Climate Projections: Atmosphere-Ocean Global Circulation Model (AOGCM)"*. [Online]
Available at: http://ukclimateprojections.metoffice.gov.uk/23213
[Accessed 15th June 2014].

UKCP, 2012c. *"UK Climate Projections: Weather Generator"*. [Online]
Available at: http://ukclimateprojections.metoffice.gov.uk/23261
[Accessed 14th June 2014].

UKCP, 2012d. *"UK Climate Projections: CDF Data"*. [Online]
Available at: http://ukclimateprojections.metoffice.gov.uk/22562
[Accessed 16th June 2014].

USGS, 2014. *"Floods: Recurrence Intervals and 100-year Floods (USGS)"*. [Online]
Available at: http://water.usgs.gov/edu/100yearflood.html
[Accessed 20th June 2014].

Warren, R., 2010. *"UK Climate Projections: Annex 1 - Emissions Scenarios Used in UKCP09"*. Exeter, UK: Met Office Hadley Centre.

Xiao, Y. Q. et al., 2006. "Probability Distributions of Extreme Wind Speed and its Occurrence Interval". *Engineering Structures,* Volume 28, pp. 1173-1181.

Xie, Q. & Sun, L., 2013. "Experimental Study on the Mechanical Behavior and Failure Mechanism of a Latticed Steel Transmission Tower". *Journal of Structural Engineering,* Volume 139, pp. 1009-1018.

Young, R. M., 2010. *"Weather Instruments - Ultrasonic Anemometer Model 85000"*. [Online]
Available at: http://www.youngusa.com/Manuals/85000-90%28J%29.pdf
[Accessed 10th July 2014].

Zhang, Z. et al., 2013. "The Numerical Analysis of Transmission Tower-Line System Wind-Induced Collapsed Performance". *Mathematical Problems in Engineering,* Volume 2013, pp. 1-11.

Appendix

Determination of Wind Loads to Eurocode 1 Part 1-4

The wind pressure (q_w) acting on a structure or structural component is computed as follows (BSI, 2005):

$$q_w = c_s c_d \, \psi_\lambda \, C_{f,\theta} \, q_p \tag{A.1}$$

Where $c_s c_d$ is the structural factor, ψ_λ the end-effect factor, $C_{f,\theta}$ the force (or drag) coefficient when wind acts at an angle θ normal to the surface without considering free-end flow and q_p the peak velocity pressure. The structural factor ($c_s c_d$) is computed for the whole structure, while the other quantities may be evaluated separately for different sections of the structure to improve the accuracy.

The force coefficient for lattice structures is a function of the solidity ratio (φ) and wind incidence angle. φ was calculated for the main body of the tower divided into six panels, plus the three arms, and values ranging from 0.128 for the bottom stage to 0.419 for the upper arm were obtained. From these, force coefficients from 3.50 to 2.15 were obtained from Figure 7.34 of BS EN 1991-1-4:2005 (BSI, 2005), taking the tower as a spatial rather than a planar structure. The force coefficient for the cables was taken as 1.20.

End effect factor ψ_λ is a function of solidity ratio and effective slenderness, λ. λ was calculated for each panel and arm of the structure, and taken as the minimum permitted value of 70 for the cables. Thus, ψ_λ calculated as 0.938 – 0.983 for the structure, and 0.925 for the cables.

The peak velocity pressure for a structure or structural component at height z from the ground level is determined as follows (BSI, 2005):

$$q_p(z) = [1 + 7I_v(z)] \, \frac{1}{2} \, \rho_{air} \, V_m^2(z) \tag{A.2}$$

Where $I_v(z)$ is the turbulence intensity, ρ_{air} the air density taken as 1.226 kg/m^3 (BSI, 2008), and $V_m(z)$ the mean wind velocity. $V_m(z)$ is the product of the basic wind velocity, roughness factor and orography factor. Assuming an area with low vegetation and isolated obstacles, such as in Figure 1 (Terrain Category II), an orography factor of 1.0 is taken. The roughness factor is evaluated using a roughness length z_0 of 0.05 m, minimum height z_{min} of 2 m and terrain factor calculated as 0.19. The basic wind velocity is calculated using directional factor of 1.0, seasonal factor of 1.0 and future wind speed from Table 3 of this paper. The partial factor for variable actions (γ_Q) was taken as 1.0.

The turbulence intensity $I_v(z)$ is calculated assuming a turbulence factor k_I of 1.0. The resulting peak velocity pressure profile for a 1 in 250 year Very Rare storm event is shown in Figure A1 (in which A-F are the stages of the tower), showing constant pressure up to a height equal to z_{min} (2 m) and then logarithmic increase with z.

The structural factor $c_s c_d$ consists of two components, size factor c_s and dynamic factor c_d. The size factor accounts for the peak wind pressures not occurring simultaneously on the whole surface, and becomes smaller as the structure size increases. The dynamic factor is an amplification factor (larger or equal to 1.0) to account for the dynamic response of the structure to wind turbulence in its fundamental (first) mode of vibration, and becomes larger as the dynamic sensitivity of a structure increases (Burgess, et al., 2010; Tubman, et al., 2010; BSI, 2005). c_s and c_d are evaluated using expressions in BS EN 1991-1-

4:2005 (BSI, 2005) that in turn utilise a number of intermediate parameters, calculated as follows:

- Reference height. For the tower, $z_{s,t} = 0.6\,H$, where H is the total height of the tower. For the cables, $z_{s,c}$ is taken as the height from the ground to the axis of the cables
- Peak factor k_p depends on the fundamental natural frequency f_1 of the structure. For the tower, this is obtained from the numerical model as 2.27 Hz. Natural frequencies of a cable can be obtained by (Ren, et al., 2008):

$$f_n = \frac{n}{2\,L_c}\sqrt{\frac{T_c}{m_c}} \tag{A.3}$$

  Where f_n is the natural frequency of the n-th mode, L_c the total length of the cable (assumed 400 m), T_c the tension in the cable and m_c the mass per unit length. A previous research study provided estimates of T_c = 23 kN and m_c = 1.71 kg/m (Newton, 2004), so that f_1 for a transmission line cable calculates as 0.15 Hz.

- Background factor (B^2) accounts for the lack of full correlation of peak wind pressures on the surface of the structure, and is described by the following expression (BSI, 2005):

$$B^2 = \frac{1}{1 + 0.9\left(\frac{B+H}{L(z_s)}\right)^{0.63}} \tag{A.4}$$

  Where B and H are the average width and total height of the structure, respectively, and $L(z_s)$ the turbulent length scale at the reference height (z_s), from the following expression (BSI, 2005):

$$L(z_s) = L_t\left(\frac{z_s}{z_t}\right)^{\alpha} \tag{A.5}$$

  Where L_t is the reference length scale taken as 300 m, z_t the reference turbulence height taken as 200 m and α taken as 0.52 for Terrain Category II.

- Resonance response factor (R^2) accounts for resonance due to wind turbulence in the fundamental (first) mode of vibration and is determined as follows (BSI, 2005):

$$R^2 = \frac{\pi^2}{2\,\zeta}\,S_L(z_s, f_1)\,R_H(\eta_H)\,R_B(\eta_B) \tag{A.6}$$

  Where ζ is the logarithmic decrement of damping, $S_L(z_s, f_1)$ the power spectral density function at the reference height (z_s) for the fundamental mode of vibration (f_1), and $R_H(\eta_H)$ and $R_B(\eta_B)$ are the aerodynamic admittance functions for the height H and average width of the structure B, respectively. ζ has two components (BSI, 2005):

$$\zeta = \zeta_s + \zeta_a \tag{A.7}$$

  ζ_s is the structural logarithmic decrement of damping, equal to 0.03 for lattice steel towers and 0.006 for cables (BSI, 2005). ζ_a is the aerodynamic logarithmic decrement of damping, defined as (Sá Caetano, 2007; BSI, 2005):

$$\zeta_a = \frac{\rho_{air}\,C_{f,0}\,V_m(z_s)}{2\,f_1\,\mu_e} \tag{A.8}$$

  Where μ_e is the mass per unit area of the structure (using plan area for the tower and cross-

sectional area for the cables).

The power spectral density function is dimensionless and described by the following expression (BSI, 2005):

$$S_L(z_s, f_1) = \frac{6.8\, f_L(z_s, f_1)}{\left(1 + 10.2\, f_L(z_s, f_1)\right)^{5/3}} \quad \text{(A.9)}$$

Where $f_L(z_s, f_1)$ is a dimensionless function of frequency related to the fundamental natural frequency f_1 (BSI, 2005):

$$f_L(z_s, f_1) = \frac{f_1\, L(z_s)}{V_m(z_s)} \quad \text{(A.10)}$$

The aerodynamic admittance functions are defined as (BSI, 2005):

$$R_x(\eta_x) = \frac{1}{\eta_x} - \frac{1}{2\,\eta_x^2}(1 - e^{-2\,\eta_x}) \quad \text{(A.11)}$$

In which:

$$\eta_x = \frac{4.6\, x}{L(z_s)}\, f_L(z_s, f_1) \quad \text{(A.12)}$$

Where x is substituted either as the height H or average width B of the structure.

By combining all the above with Equation (A.2), the wind pressure profile for the entire height of the tower can be obtained. The wind pressure profile for *RI* = 250 years is shown in Figure A2, where again A-F are the stages of the main body of the tower, and LA, MA and UA the lower, middle and upper arms respectively.

Table 1: PBWE Framework (adapted from SEAOC, 1999)

Hazard Level (HL)	Performance Objective (PO)			
	Fully Operational	Operational	Damage Control	Near Collapse
	Repairable Damage		Non-Repairable Damage	
Frequent (2 - 3 years)	Normal	Unacceptable	Unacceptable	Unacceptable
Occasional (10 years)	Essential	Normal	Unacceptable	Unacceptable
Rare (50 - 100 years)	Safety Critical	Essential	Normal	Unacceptable
Very Rare (250 years)	-	Safety Critical	Essential	Normal
Maximum Considered (500 - 1000 years)	-	-	Safety Critical	Essential

Table 2: Weibull parameters and hourly mean wind speeds for the baseline and future time periods (medium A1B emissions)

k	$\overline{V}_{b,max}\ [m/s]$	$c_b\ [m/s]$	$\overline{V}_{p,max}\ [m/s]$	$c_p\ [m/s]$
1.28	11.54	12.45	11.74	12.67

Table 3: Future hourly wind speeds for different Hazard Levels (NE England, medium emissions scenario)

Hazard Level	Frequent	Occasional	Rare	Very Rare	Maximum Considered
Recurrence Interval [$years$]	**2.5**	**10**	**50 – 100**	**250**	**500 – 1000**
Baseline Wind Speed [m/s]	11.6	23.9	36.2 – 41.1	47.3	51.9 – 56.4
Future Wind Speed [m/s]	12.2	25.3	38.3 – 43.5	50.2	55.1 – 59.7

Table 4: Future 10-minute wind speeds for different recurrence intervals (NE England, medium emissions scenario)

Hazard Level	Frequent	Occasional	Rare	Very Rare	Maximum Considered
Recurrence Interval [$years$]	**2.5**	**10**	**50 – 100**	**250**	**500 – 1,000**
Future Wind Speed [m/s]	13.1	27.1	40.9 – 46.5	53.7	58.9 – 63.9

Table 5: Load factors from materially and geometrically nonlinear analyses

Type of Analysis	Load factor as function of Hazard Level and Wind Direction					
	Rare $RI = 50$ years		Very Rare $RI = 250$ years		Maximum Considered $RI = 500$ years	
	0°	45°	0°	45°	0°	45°
MNL	2.04	1.12	1.18	0.66	0.96	0.56
MGNL	1.36	1.06	0.79	0.63	0.66	0.52

Table 6: Load factors obtained in linear eigenvalue buckling analyses

Global Mode	Linear Buckling Load Factor as function of Hazard Level and Wind Direction					
	Rare $RI = 50$ years		Very Rare $RI = 250$ years		Maximum Considered $RI = 500$ years	
	0°	45°	0°	45°	0°	45°
1	1.99	1.70	1.16	1.00	0.97	0.83
2	2.19	1.76	1.28	1.04	1.07	0.86

Table 7: Summary of transmission tower performance for different Hazard Levels

Hazard Level (Return Period)	Performance Level			Performance Assessment Satisfied
	Minimum Required	MGNL Analysis	Linear Buckling Analysis	
Rare (50 years)	Operational (Slight Damage)	Fully Operational (No Damage)	Fully Operational (No Damage)	✓
Very Rare (250 years)	Damage Control (Moderate/Heavy Damage)	Damage Control (Heavy Damage)	Operational (Slight Damage)	✓
Max. Considered (500 years)	Near Collapse (Severe Damage)	Near Collapse (Severe Damage)	Near Collapse (Severe Damage)	✓

Figures

Figure 1: Damaged electricity pylon near Houghton-le-Spring, UK (BBC News, 2014)

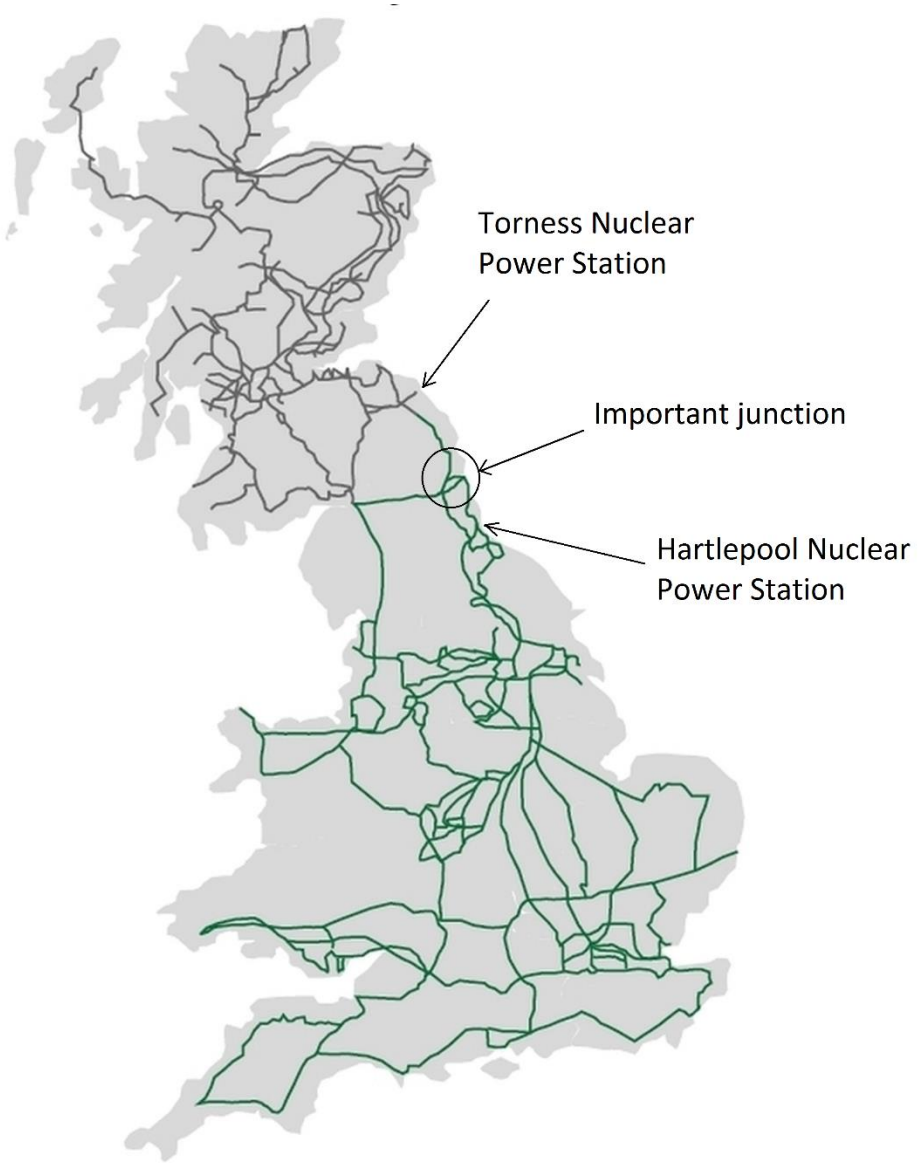

Figure 2: Electricity transmission networks of Great Britain (adapted from UK Parliament, 2010)

Figure 3: D L6 Blaw Knox type suspension tower located in Dorset, UK (Hendry, 2005)

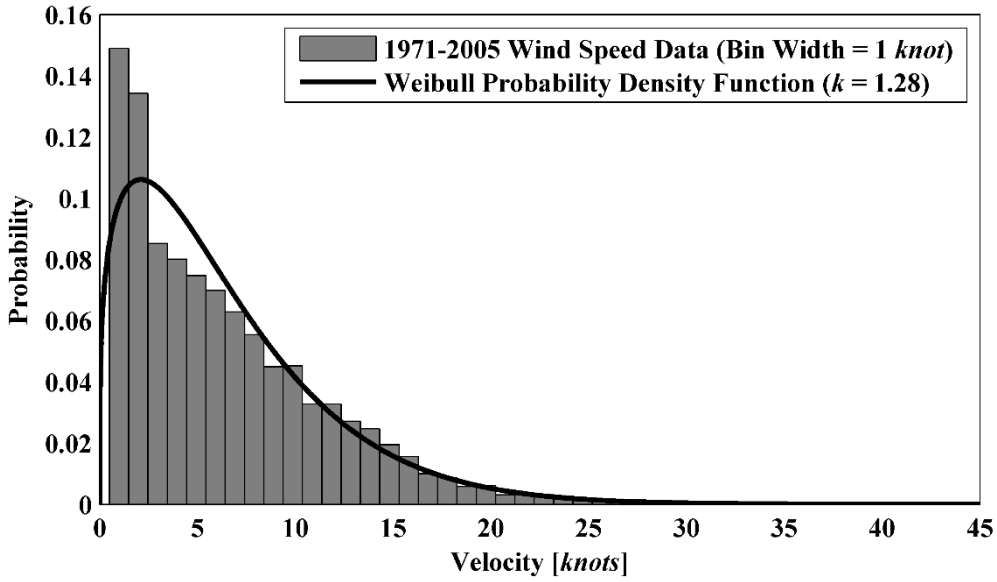

Figure 4: Weibull distribution fit to recorded hourly mean wind speed data for Durham 1971-2005

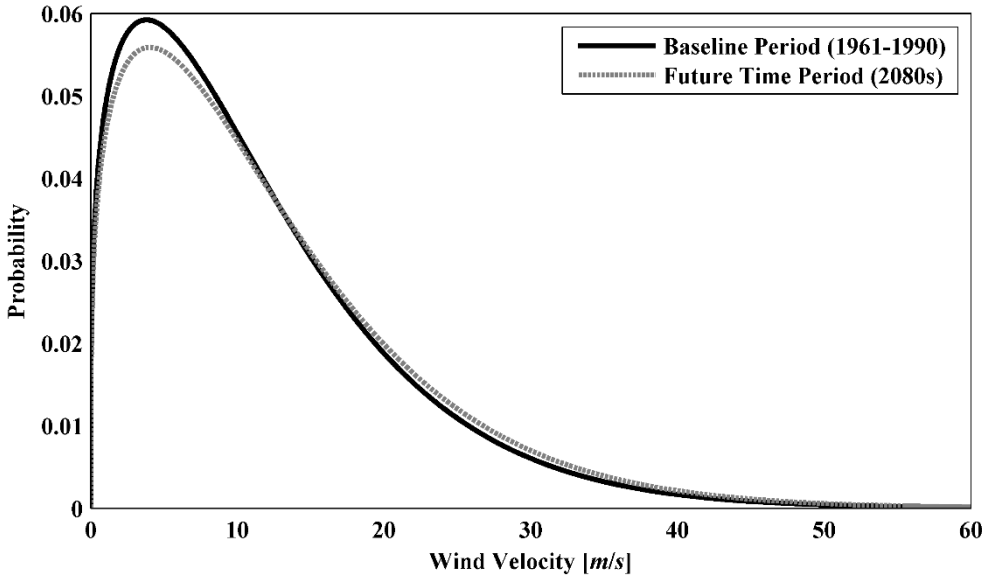

Figure 5: Weibull probability density functions for hourly mean wind velocity for NE England, baseline and future time periods (medium A1B emissions)

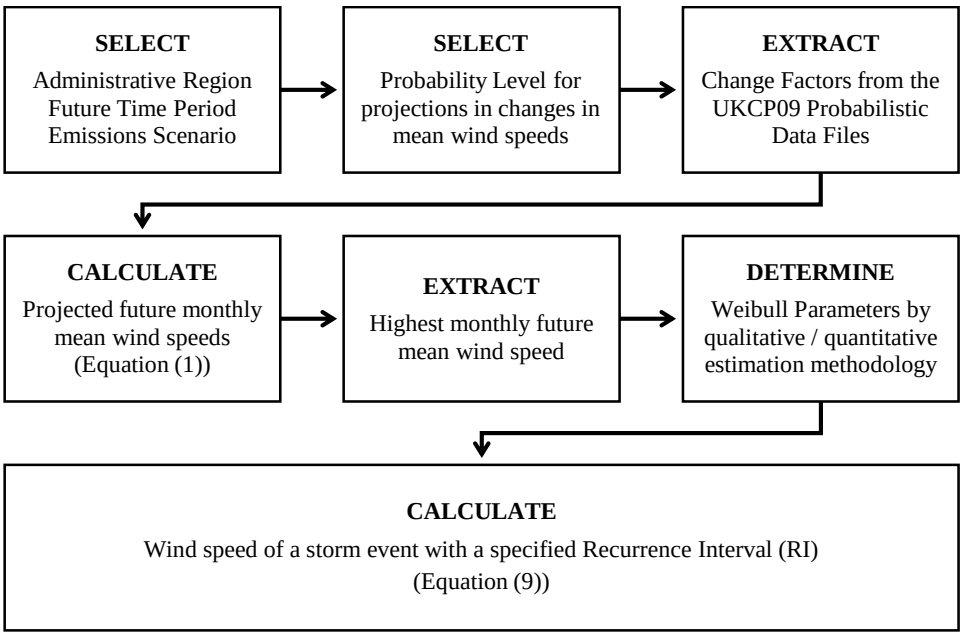

Figure 6: Flowchart of methodology used for determination of magnitude of future storm events

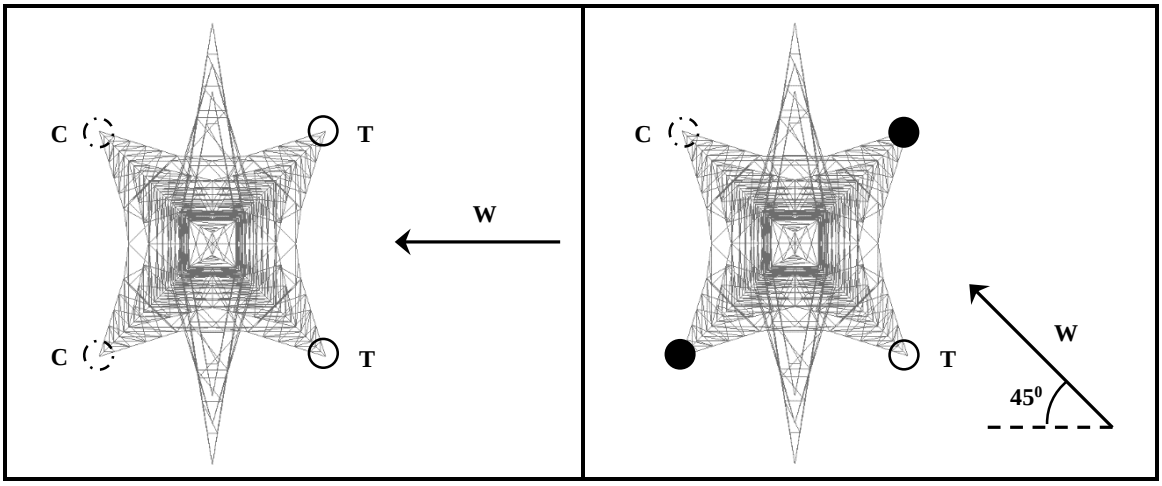

Figure 7: Stress state (T: Tension / C: Compression) of the main leg members for two wind incidence angles

Figure 8: Comparison of the orientation of the main and diagonal leg members in the real structure and numerical model

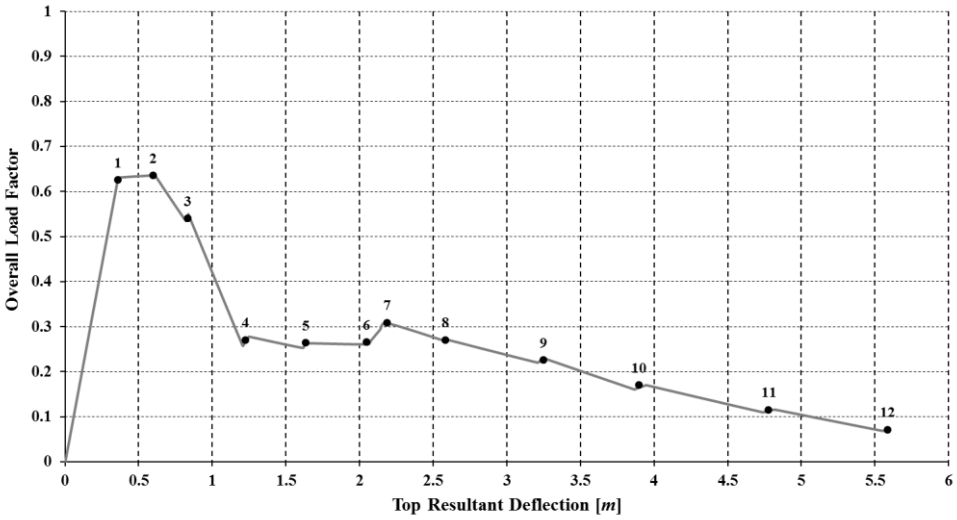

Figure 9: Pushover curve for a 1 in 250 year storm event and 45° wind incidence angle

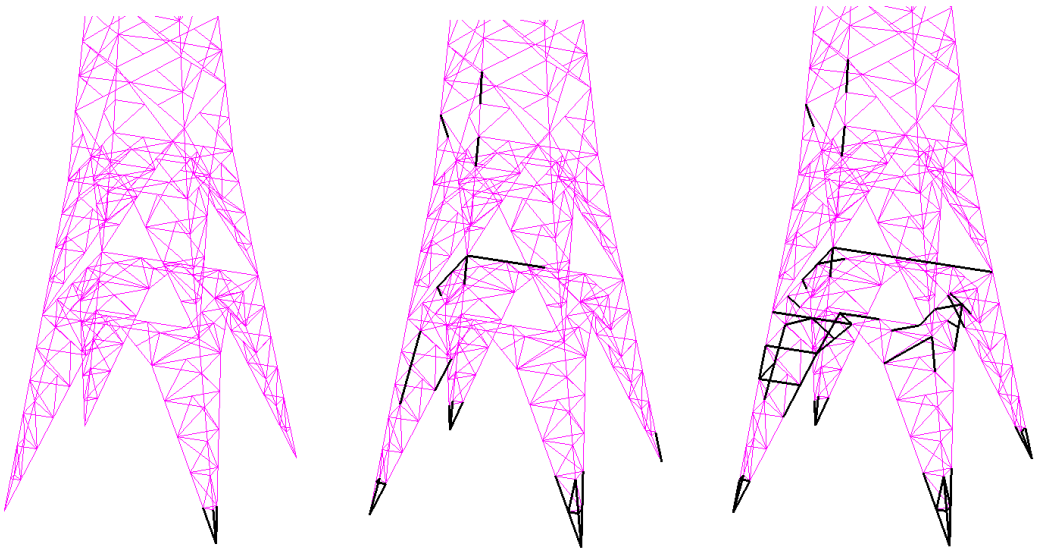

Figure 10: The evolution of plastic yielding in the structural members (Points 2, 7 and 11)

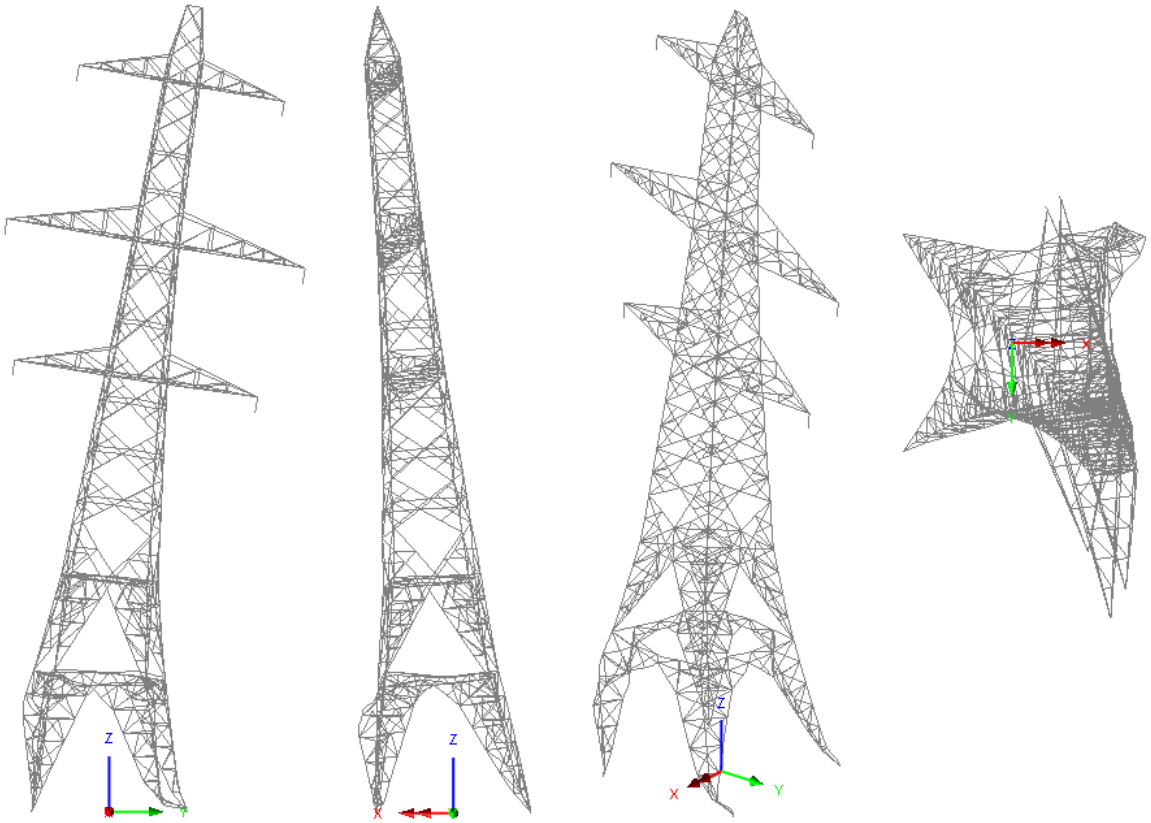

Figure 11: Deformed shape at end of pushover analysis for Very Rare storm event and 45° wind incidence angle

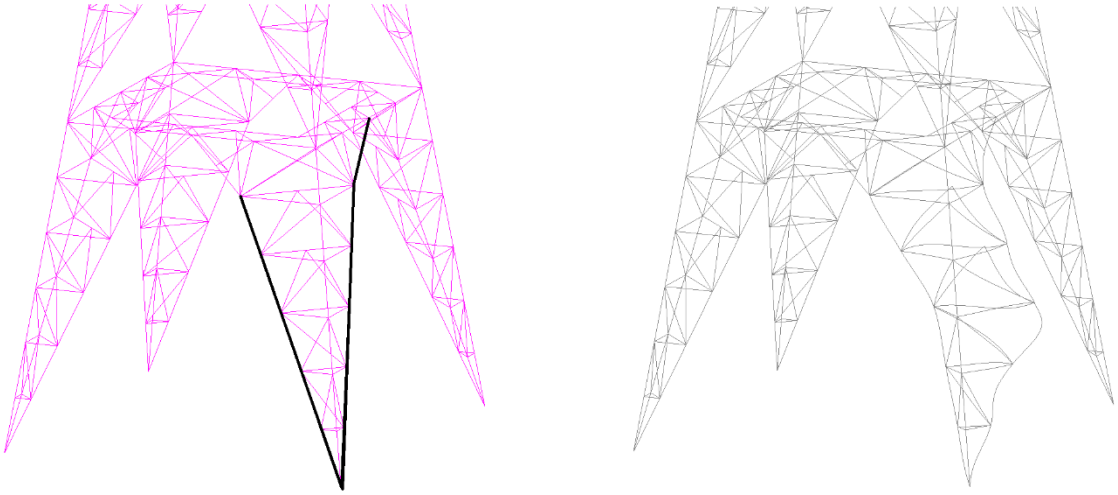

Figure 12: Critical buckled members (left) and deformed shape (right) for the 1st global model

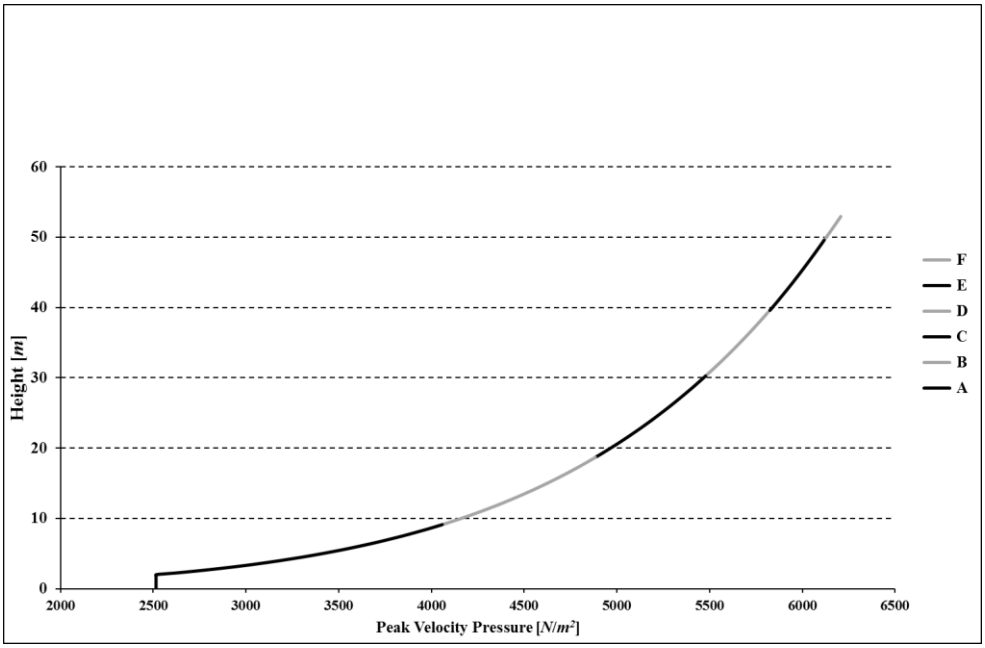

Figure A1: Peak velocity pressure profile for a 1 in 250 year storm event

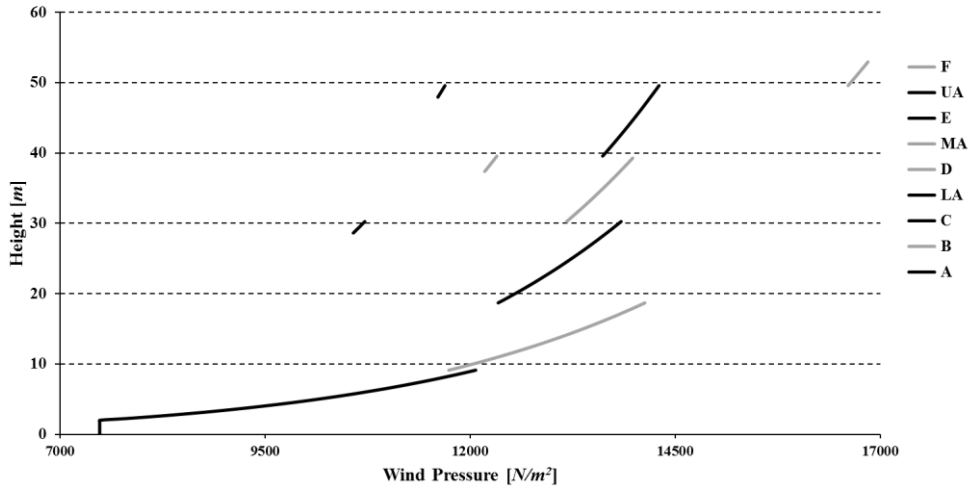

Figure A2: Wind pressure profile for a 1 in 250 year storm event